International Journal of GEOMATE, Jan., 2020, Vol.18, Issue 65, pp. 86-93
ISSN: 2186-2982 (P), 2186-2990 (O), Japan, DOI: https://doi.org/10.21660/2020.65.54094
Geotechnique, Construction Materials and Environment

MEASURING STRAINS ON GEOGRID SPECIMENS UNDER THE LABORATORY TENSILE TEST

*Chamara Prasad Gunasekara Jayalath[1] and Kasun Dilhara Wimalasena[2]

[1,2] School of Civil Engineering and Built Environment, Queensland University of Technology, Australia

*Corresponding Author, Received: 27 Oct. 2019, Revised: 08 Nov. 2019, Accepted: 28 Nov. 2019

ABSTRACT: Geosynthetic products such as geogrids act a key role in geotechnical engineering as they are widely used in reinforcing pavement materials, embankments and retaining wall backfills. Therefore, measuring strains in geogrids is vital to evaluate their performances in geogrid-reinforced structures and, to determine their strength parameters such as secant stiffness and tensile strength. However, verifying the measured strain is required as these strains are affected by several factors including the gauge factor, data logging device, temperature and the quality of bonding between strain gauge and geogrid. Therefore, this research was conducted to verify the performance of strain gauges attached to geogrids and also to investigate the possibility of using Particle Image Velocimetry (PIV) technique and GeoPIV-RG software to measure the local strains developed in geogrid specimens under tensile testing in the laboratory. In this experimental study, a wide-width tensile test was conducted on composite geogrid test specimens while calculating/measuring its tensile strain by three methods, namely, using Geo-PIV-RG analysis, strain gauges attached to the specimens, and crosshead movements of Instron apparatus. Test results showed that there is a significant agreement between the strains obtained from strain gauges and GeoPIV-RG analysis for all the tests conducted. Therefore, it can be concluded that the PIV technique along with GeoPIV-RG program can be effectively used to measure the local strain of geogrids in the laboratory tests. In addition, properly installed strain gauges can be used in the field applications to measure strains in the geogrids.

Keywords: PIV analysis, Strain gauge, Geogrid, Wide-width tensile test, Tensile strength

1. BACKGROUND

Nowadays, geotechnical engineers face numerous challenges including difficulties in incorporating unsaturated soils [1-3] and expansive soils [4, 5] into routine geotechnical engineering designs and constructions, scarcity of quality pavement construction materials in hauling distance, and limited financial resources [6]. It has been identified that chemical stabilization of pavement material [7], and using recycled materials [8-11] and geosynthetic products [6] in geotechnical construction are the most popular methods utilized to overcome the above-mentioned challenges. Geosynthetic products act a key role in geotechnical engineering as they are widely used in reinforcing pavement materials, embankments and retaining wall backfills. In addition, geosynthetic products can be used to enhance the performance and service life of railways [12], coastal engineering applications [13-15] and also as hydraulic barriers for waste containment facilities, water retention systems and mining applications [16,17]. The main functions of geosynthetic materials are separation, filtration, reinforcement, stiffening, drainage, hydraulic or gas barrier and protection [18].

It has been recognized that inclusion of composite geogrids which are the geogrids combined with a nonwoven geotextile component, into the pavement structure maximizes the benefits of geosynthetic-reinforcement in flexible pavements. In this context, evaluating the strain behaviour of composite geogrid under tensile load is required to develop numerical models that can be used to predict the behaviour of geogrid-reinforced flexible pavements [19]. Similarly, it is vital to evaluate their performances in geogrid-reinforced structures and, to determine their strength parameters such as secant stiffness and tensile strength. It is well known that wide-width tensile test [20] is generally used to characterize the strain-stress properties of these materials.

It is essential to continuously measure the strain development of geosynthetics during the tensile test for a better understanding of the tensile behaviour of the material. In general, the average developed strain within the test specimen is computed considering the relative displacement between the two grips. However, this strain measurement method is incapable of measuring the local strains developed within the sample due to the presence of seam, production defects, punctured zones or tear of the geosynthetic product which can be significantly affected by its behaviour under tensile load [21, 22]. Similarly, the computed strains are influenced by the slippage of the test specimens in the clamps. Therefore, it is recommended to measure strains over a central portion of the test specimen instead of using the crosshead displacement [23].

Strain gauges are widely used in measuring local strains of test specimens; however, the measured strains are known to be slightly different from the actual strains as these sensors stiffen the geosynthetic material [19]. Further, measured strains are affected by the data logging device, gauge factors, quality of bonding between strain gauge and geogrid, and temperature. In addition, careful attention to surface preparation and gluing is required when strain gauges are glued on test specimens. Apart from that, strain gauges easily detach from the specimen surface at large strains well before the rupture of the test specimen [23]. Further, it is an expensive option to use when more strain gauges are needed. In addition, a difference between the strain measured by the foil strain gauge and the actual local strain at the same location of the test specimen can be existed due to the above-mentioned drawbacks; hence, the calibration is necessary to verify the performance of strain gauges. Therefore, to overcome these shortcomings of strain gauges, image-based approach such as Particle Image Velocimetry (PIV) can be used to measure the local strain of geosynthetic specimens during the tensile testing, and also verify the performance of strain gauges.

The PIV technique along with GeoPIV-RG software has been successfully used to analyze the images from a model test conducted to investigate the punch-through of a flat footing with 30mm diameter [24]. In addition, GeoPIV-RG program was used to analyze the local strains developed in nonwoven geotextile during the wide width tensile testing [25]. However, no significant research study has been conducted to verify the applicability of this image-based technique for measuring localized strain in any type of geogrid, comparing the strain gauge measurements. Therefore, this research was conducted to verify the performance of strain gauges and to investigate the possibility using PIV technique and GeoPIV-RG software to measure the local strains developed in composite geogrid specimens under tensile testing in the laboratory.

2. PIV TECHNIQUE

Digital Image Correlation (DIC) method is a widely accepted and commonly used surface deformation measurement technique, and this method is considered as a powerful and flexible tool to measure strains [26]. It is well known that PIV is a special class of the DIC method. The PIV method has been successfully used in previous research studies to measure strain on test specimens [27]. In principle, this technique will accurately predict strains, clearly identifying the provided ‘particles’ (of specific colour and texture) by the algorithm, which depends on the quality of the digital image captured during the experiment [28]. The same authors further explained that appropriate shutter speed, light level and focus must be maintained, and the camera should be kept remain stationary on a firm tripod with no manual interference. Therefore, a computer is used for triggering the shutter opening.

The basic principle of DIC/PIV technique is that tracking the same points (or pixels) between un-deformed (or reference) and deformed states as schematically illustrated in Fig.1. The DIC/PIV method is considered as optical metrology which involves both digital image processing and numerical computation. The surface strain field in the vertical direction (the direction of applied tensile force) can be determined from Eq. (1) [28].

Generally, in PIV analysis, a region of interest (RoI) should be first defined on the initial/reference image. Then a mesh with patches (or subsets) of user-defined size is created. Freely available PIV–DIC software such as MatPIV [29], GeoPIV [30], OpenPIV [31] and PIVlab [32] can be used to analyse images. A form of cross-correlation is used in these software programs to obtain integer pixel displacements, and subpixel of the correlation peak is interpolated. However, these algorithms are based on “zero-order deformation” which means the deformations of subsets are not generally allowed. Therefore, a correlation between subsets is lost in regions where large deformations are experienced caused by a mismatch between the deformation being observed and the subset shape. However, an update of the GeoPIV program called GeoPIV-RG eliminates this issue as it incorporates higher-order (first-order) subset shape functions [24].

(a)

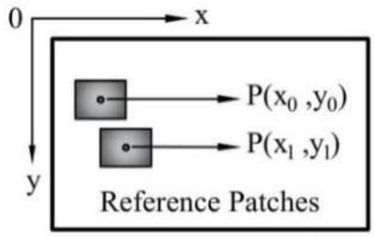

(b)

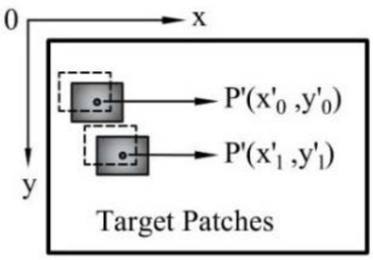

Fig.1 The basic principle in PIV analysis [28]; (a) Reference Image; (b) Deformed Image

$$\varepsilon_{yy} = \partial u_y/\partial y = \{(y_1^{/} - y_0^{/})-(y_1 - y_0)\}/ (y_1 - y_0) \qquad (1)$$

where ε_{yy} is the surface strain field in the direction of applied tensile force.

3. MATERIALS AND STRAIN GAUGES

3.1 Geogrid

As shown in Fig.2, a composite geogrid made of Polypropylene was used in this research study. The properties of composite geogrid for both Machine Direction (MD) and Cross Machine Direction (CMD) provided by the manufacturer are shown in Table 1. The nominal strength of the composite geogrid is 40kN/m in both directions.

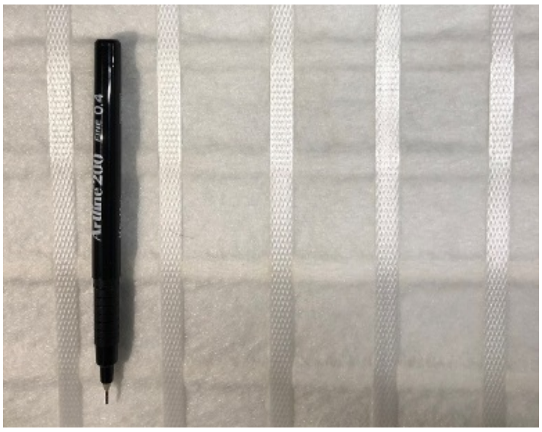

Fig.2 Composite geogrid

Table 1: Properties of composite geogrid

Property	Units	MD/CMD
Geogrid		
Maximum Tensile Strength	kN/m	≥ 40/ ≥ 40
Elongation at Nominal Strength	%	≤ 8/ ≤ 8
Tensile Strength at 2% Elongation	kN/m	16/16
Tensile Strength at 5% Elongation	kN/m	32/32
Aperture Size	mm	31/31
Geotextile		
Maximum Tensile Strength	kN/m	7.5/11
Elongation at Maximum Tensile Strength	%	40/30

.

3.2 Strain Gauges

Two types of strain gauges were used in this experimental program. A three-wire quarter-bridge strain gauge (SG1) (Fig.3 (a)) was used to verify its performance by comparing it with strain calculated from PIV analysis. This type of strain gauge has a Gauge Factor (GF) of 2.11 at 20 ^{0}C and the arm resistance of 120Ω and it is suitable for measuring strains on materials such as plastic which has low elastic modulus compared to metal. In wide-width tensile testing, strain gauges (SG2) (Fig.3 (b)) were used to measure localised strains on composite geogrid test specimens. They have constantan metal foil grids with 120 Ω arm resistance and the gauge factor of 2.14 at 20 ^{0}C. This gauge has flexible polyimide backings and the copper coated solder tabs.

4. METHODOLOGY

The testing program consists of two phases. The performance verification of strain gauges was conducted in the first phase using a strain gauge attached to a composite-geogrid strip with a single rib. In the second phase, wide-width tensile tests were carried out according to BS EN ISO 10319:2015 on the composite geogrid test specimens attached with strain gauges. The constant strain rate of 10% per minute was applied for all geogrid tensile tests.

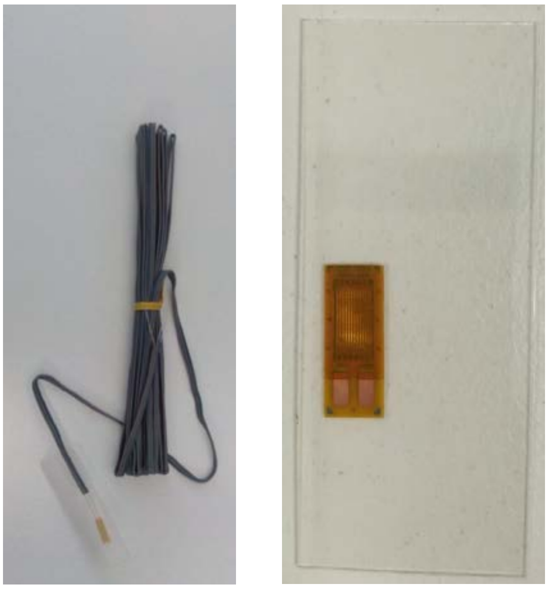

(a) (b)

Fig.3 Strain gauges used in this experimental study; (a) SG1; (b) SG2

4.1 Verification of strain gauge performance using a single rib geogrid strip

Firstly, a 130mm long and 57mm wide composite geogrid specimen having a 7.5mm wide single rib was prepared and a standard strain gauge (SG1) was glued in the middle of the specimen in the direction of applied tensile force. Then the coating of the stain gauge was done in such a way that the first coating is with SB tape and the final coating is with VB tape (See Fig.4). The purpose of the application of these coatings is to replicate the installation procedure of strain gauges on geogrids which will be used as soil reinforcements in civil engineering applications such as pavements and reinforced backfills. These coatings are used to protect the strain gauges from moisture and gravel particles. A resistor equal to the arm resistance of the strain gauge (120Ω) was used as a bridge completion resistor with the strain gauge to balance the bridge.

To perform PIV analysis, dots with the diameter of 2mm were marked on the rib of the composite geogrid as shown in Fig.5. Dots were marked using a permanent marker in such a way that the gap between two consecutive dots was less (approximately 5mm) near the strain gauge and larger (approximately 10mm) for other locations. Then, the geogrid specimen was set up in the Instron Universal Testing System (the capacity is 50kN) as shown in Fig.5. The specimen was subjected to a monatomic tensile force by applying a constant strain rate of 10% per minute. During the test, photographs were taken every five seconds using a Digital Single Lens Reflex (DSLR) camera properly p ental setup as shown in

Fig.4 The single-rib-geogrid-strip with an attached strain gauge (SG1)

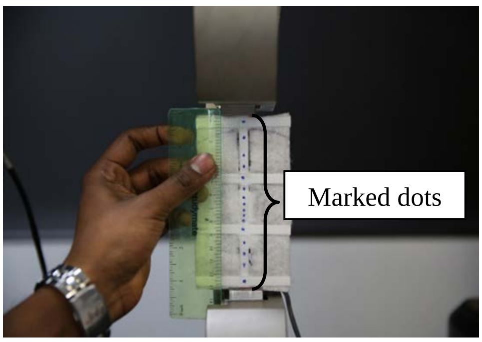

Fig.5 The single-rib-geogrid-strip set up in the Instron Universal Testing System

During the test, the strain gauge responses were recorded for every second using a data logger. The data logger was set to calculate strains using the gauge factor and the response of the strain gauge. The global strain on the geogrid specimen was calculated considering the recorded extension values (crosshead movement) by the Instron Universal Testing System and the initial length of the test specimen. The photographs taken during the test were analyzed using Geo-PIV-RG software to calculate the local strains (using Equation 1) in the region where the strain gauge was attached. At the end of the test, the strains measured by the strain gauge, calculated from Geo-PIV-RG analysis and calculated from the movement of the crossheads of the Instron apparatus were compared.

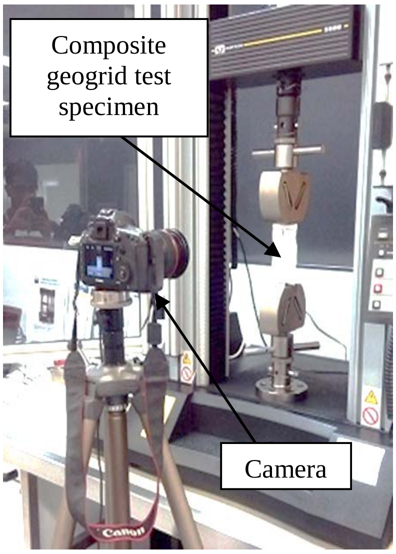

Fig.6 Taking photographs for PIV analysis

4.2 Wide-width tensile testing

Six test specimens were prepared in such a way that the width is 200mm and the length between the jaws is 100mm. A SG2 was glued on each specimen in the direction of the applied tensile force. Dots were marked at the centre and junctions of each rib of test specimens using a permanent marker as shown in Fig.7. The test geogrid specimen was clamped in the Instron Universal Testing System as in Fig.7 and the tensile test was conducted according to BS EN ISO 10319. All tests were conducted with a constant strain rate of 10% per minute until the failure (break) of geogrids. During each test, the strains were measured/calculated using all three methods described in section 4.1. In all tests, strain gauges failed or detached before reaching 1% of strain.

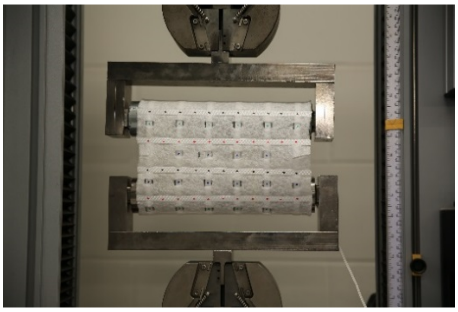

Fig.7 A test specimen under wide-width tensile test

5. Results and Discussion

Fig.8 shows the load versus strain curves obtained from the tensile test on the single rib geogrid strip. Depending on the technique (e.g: strain gauge, PIV analysis, machine displacement) used to measure/calculate strain during the test, three curves are produced as shown in Fig.8. All three curves are produced up to the strain of 0.009 (0.9%) as the strain gauge failed to respond after 0.9% of strain. The local strain measured by the strain gauge agrees well with that of calculated from the GeoPIV-RG analysis at the same location of the strain gauge. From the results shown in Fig.8, it can be suggested that both the GeoPIV-RG analysis and properly installed strain gauges can measure local strains accurately. However, the accuracy of the strains measured by the strain gauges depends on several factors that have been discussed in section 1 (Introduction). Therefore, the GeoPIV-RG analysis can be used as an economical and reliable method to measure the strain in geogrids when testing them for the tensile strength and stiffness in the laboratory. Carefully chosen, properly installed and, correctly logged strain gauges can be used to measure strains in geogrids which are installed in the field.

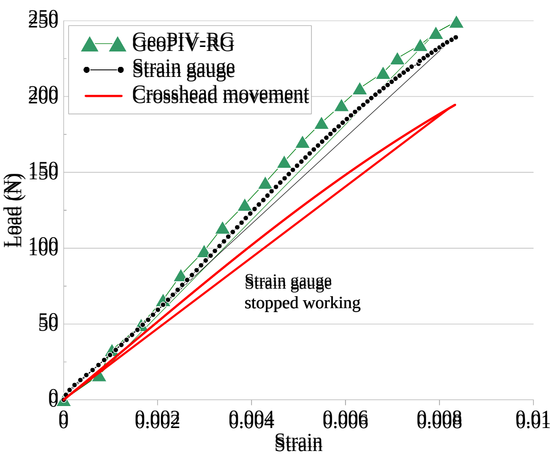

Fig.8 Load vs Strain curves obtained from tensile on the single rib geogrid strip

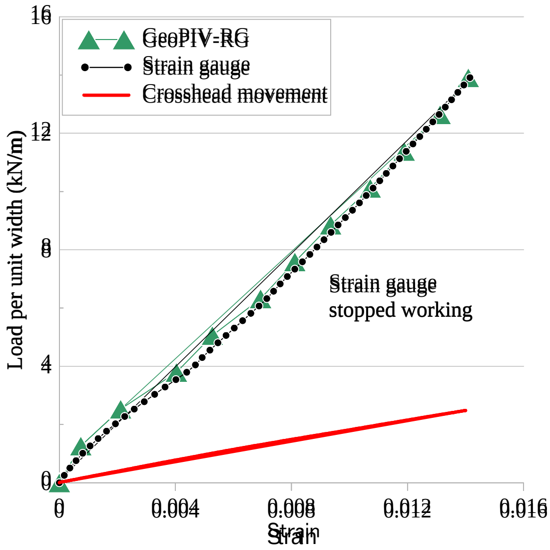

(a)

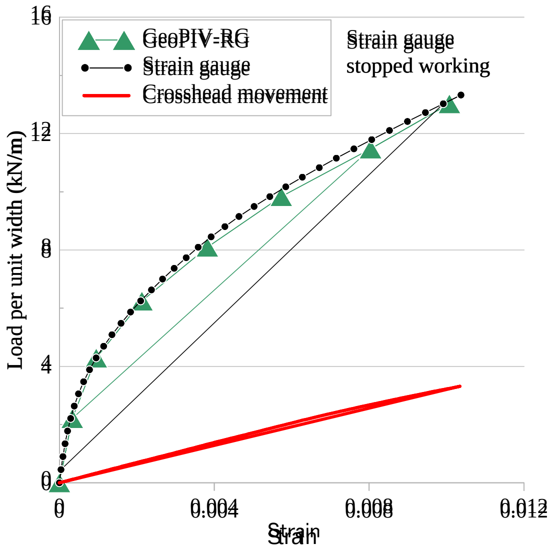

(b)

Fig.9 Load per unit width - strain curves for two wide-width tensile test specimens; (a) Test 1; (b) Test 2

Fig.9(a) and 9(b) depict load (per 1m width) vs strain curves obtained from two wide-width tensile tests on composite geogrid specimens. These results further confirm that both strain gauges and the GeoPIV-RG analysis can be used to measure local strain on geogrids accurately. The results shown in Fig.8 and 9 suggest that the GeoPIV-RG analysis can be used to verify the performance of strain gauges attached on geogrids. So this type of verification test can be used to choose suitable strain gauges, to identify strain gauge installation procedure, and to choose and set up data logging for measuring strains on geogrids installed in the field applications. The GeoPIV-RG analysis can successfully be used to measure strain in the laboratory tensile tests on geogrids when one has to measure strain more than 3% with a limited budget and less time consumption.

As shown in Fig.8 and 9, the strain calculated from the crosshead displacement of the loading machine underestimate the tensile stiffness of geogrid. This technique calculates the overall strain of the specimen and it is generally much higher than the values measured/calculated locally by strain gauges or GeoPIV-RG analysis at a given load. The reason for this mismatch is the crosshead displacement measured by the loading machine can include machine deformation, slippage of the specimen at gripping points and the boundary effects at the grips.

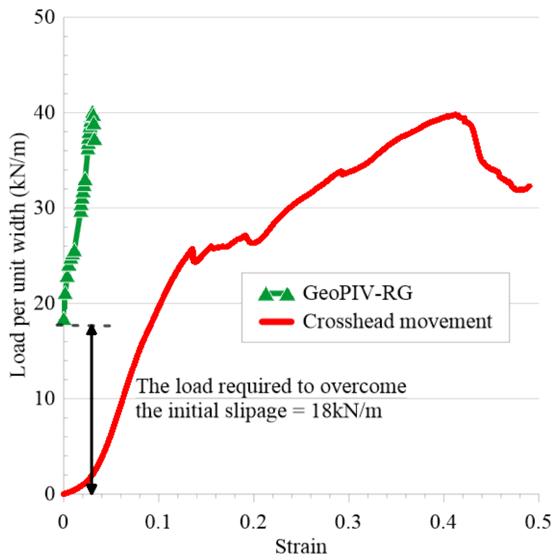

Fig.10 Load per unit width/strain curve up to the failure of the geogrid specimen

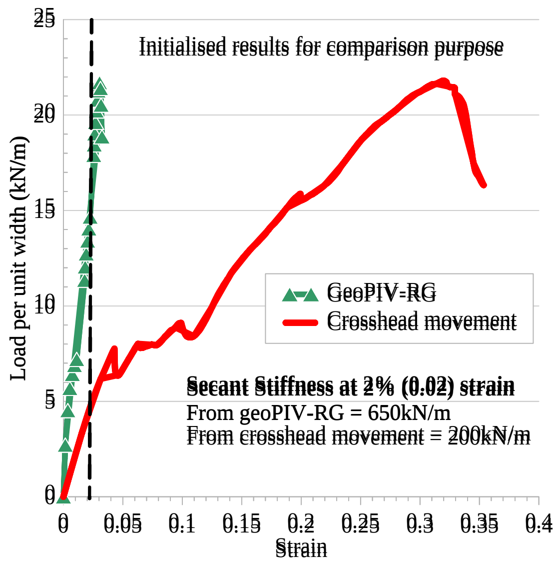

Fig.11 Comparison of secant stiffness

Fig.10 shows load (per 1m width) vs strain curves obtained from a wide-width tensile test on a composite geogrid specimen used. Strains were calculated using crosshead deformation of the tensile testing machine and using GeoPIV-RG technique until the failure (rupture) of the test specimen. The maximum tensile strength (rupture strength) is measured as about 40kN/m and it is well agreed with the value given in the material specification (Table 1). In the PIV analysis, strains calculated up to about 18kN/m load showed negative strains with continuous increment which indicated the possible slippage of the test specimen in the initial stage of the test. However, the occurred slippage cannot be observed through the strain calculated from the crosshead movement as the Instron machine constantly maintains the 10% strain rate. Therefore, the GeoPIV-RG technique provides a better representation of actual strain variation within geogrid specimens compared to the crosshead movement method.

As shown in Fig.11, the tensile load and the strain values were initialised the variation of load per unit width with strain was plotted in such a way that the secant modulus from GeoPIV-RG technique and crosshead-movement method can be calculated. Fig.11 shows that the tensile strength values at 2% are approximately 13kN/m and 4kN/m from GeoPIV-RG analysis and crosshead movement of the apparatus, respectively. The material specification (Table 1) provides the tensile strength at 2% strain as 16kN/m. Further, using the load-strain curves given in Fig.11, the scant stiffness of geogrid at 2% is calculated as 650kN/m and 200kN/m from load-strain curves obtained using GeoPIV-RG analysis and crosshead deformation of the machine, respectively. It is clear from these results that the strains calculated from the movement of the crossheads of the tensile testing machine significantly under-estimate the tensile properties of the geogrid. Therefore, GeoPIV-RG can be suggested as a strain measuring technique in laboratory tensile tests on geogrids to determine their tensile properties accurately.

6. CONCLUSIONS

The experimental study discussed in this research paper presented the way GeoPIV-RG analysis can be utilised to verify the performance of strain gauges attached on geogrid specimens. Similarly, it emphasised the benefits of using GeoPIV-RG technique to measure strain variation in geogrid specimens under the laboratory tensile tests. The following conclusions can be drawn from this research study:

Both properly installed strain gauges and GeoPIV-RG technique are capable of accurately measuring local strains on geogrid specimens under tensile force.

GeoPIV-RG analysis can be used to verify the performance of strain gauges attached to geogrid specimens.

GeoPIV-RG is a low-cost strain measuring technique that can be used in laboratory tensile testing on geogrid specimens to determine their tensile properties accurately.

For monitoring the field performance of a given geogrid type, suitable strain gauges along with the correct installation procedure and effective data logging systems can be suggested. This is due to the reason that applying PIV technique for measuring local strains of geogrid specimens is not possible in the field applications.

7. ACKNOWLEDGMENTS

The authors acknowledge the continued support of the Department of Transport and Main Roads (TMR) and Australian Road Research Board (ARRB) by providing the required funding for the instruments including data logger and strain gauges for this research study and supplying the composite geogrid material. Thanks are also extended to the technical staff of Queensland University of Technology (QUT) for their great support and assistance during these tests. Further, the authors would like to thank QUT for providing scholarships to pursue their postgraduate studies.

8. REFERENCES

[1] Gallage, C., Udukumburage, R., Uchimura, T., and Abeykoon, T., Comparison of direct and indirect measured soil-water characteristic curves for a silty sand. International Journal of GEOMATE, 13(39), 2017, 9-16.

[2] Gallage, C., Dareeju, B., Dhanasekar, M., and Ishikawa, T., Effects of principal stress axis rotation on unsaturated rail track foundation deterioration. Procedia engineering, 143, 2016, 252-259.

[3] Gallage, C., Kodikara, J., and Uchimura, T., Laboratory measurement of hydraulic conductivity functions of two unsaturated sandy soils during drying and wetting processes. Soils and Foundations, 53(3), 2013, 417-430.

[4] Jayalath, C. P. G., Gallage, C., and Miguntanna, N. S., Factors affecting the swelling pressure measured by the oedemeter method. International Journal of Geomate, 11(24), 2016, 2397-2402.

[5] Gallage, C. P. K., Kodikara, J., and Chan, D., Response of a plastic pipe buried in expansive clay. Proceedings of the ICE-Geotechnical Engineering, 165(1), 2011, 45-57.

[6] Jayalath, C. P. G., Gallage, C.P, Dhanasekar, M., Dareeju, B.S., Ramanujam, J.M. and Lee, J., [2018] Pavement model tests to investigate the effects of geogrid as subgrade reinforcement, Proceedings of the 12th Australian and New Zealand Young Geotechnical Professionals Conference, p1-8.

[7] Dang, L. C., Hasan, H., Fatahi, B., Jones, R., and Khabbaz, H., Enhancing the engineering properties of expansive soil using bagasse ash and hydrated lime. International journal of GEOMATE, 11(25), 2016, 2447-2454.

[8] Jayakody, S., Gallage, C., and Ramanujam, J., Effects of reclaimed asphalt materials on geotechnical characteristics of recycled concrete aggregates as a pavement material. Road Materials and Pavement Design, 20(4), 2019, 754-772.

[9] Clark, B. R., Gallage, C., and Yeaman, J., Temperature susceptibility of multigrade bitumen asphalt and an approach to account for temperature variation through deep pavements. International Journal of Urban and Civil Engineering, 12(6), 2018, 712-717.

[10] Clark, B. R., Piacere, L., and Gallage, C., Effects of Recycled Asphalt Pavement on the Stiffness and Fatigue Performance of Multigrade Bitumen Asphalt. Journal of Materials in Civil Engineering, 30(2), 2017, 04017278.

[11] Jayakody, S., Gallage, C., and Kumar, A., Assessment of recycled concrete aggregates as a pavement material. Geomechanics and Engineering, 6(3), 2014, 235-248.

[12] Askarinejad, H., Barati, P., Dhanasekar, M., and Gallage, C., Field studies on sleeper deflection and ballast pressure in heavy haul track. Australian journal of structural engineering, Vol. 19(2), 2018, pp. 96-104.

[13] Cheah, C., Gallage, C., Dawes, L., and Kendall, P., Impact resistance and evaluation of retained strength on geotextiles. Geotextiles and Geomembranes, Vol. 44(4), 2016, pp. 549-556.

[14] Cheah, C., Gallage, C., Dawes, L., and Kendall, P., Measuring hydraulic properties of geotextiles after installation damage. Geotextiles and Geomembranes, Vol. 45(5), 2017, pp. 462-470.

[15] Cheah, C., Gallage, C., Dawes, L. A., and Kendall, P., Effect of simulated rock dumping on geotextile, In Ramsay, Graham (Ed.) 12th Australian New Zealand Conference on Geomechanics (ANZ 2015), 2015, Wellington, New Zealand.

[16] Weerasinghe, I. A., Gallage, C., and Dawes, L., Optimising geosynthetic clay liner overlaps: Implications on hydraulic performance.

Environmental Geotechnics, 2019.
[17] Weerasinghe, I. A., Gallage, C. P. K., Dawes, L., and Kendall, P., Liquid flow mechanism at a geosynthetic clay-liner overlap, In Geosynthetics 2019, 2019, Houston, TX.
[18] Zornberg, J. G., Functions and applications of geosynthetics in roadways. Procedia engineering, 189, 2017, pp. 298-306.
[19] Warren, K. A., Christopher, B., and Howard, I. L., Geosynthetic strain gage installation procedures and alternative strain measurement methods for roadway applications. Geosynthetics International, Vol. 17(6), 2010, pp. 403-430.
[20] ISO, EN. 10319: Geosynthetics Wide-width Tensile Test. 2015, International Organization for Standardization, Geneva, Switzerland.
[21] Aydilek, A. H., Guler, M., and Edil, T. B., Use of image analysis in determination of strain distribution during geosynthetic tensile testing. Journal of Computing in Civil Engineering, Vol. 18(1), 2004, pp. 65-74.
[22] Kutay, M. E., Guler, M., and Aydilek, A. H., Analysis of factors affecting strain distribution in geosynthetics. Journal of geotechnical and geoenvironmental engineering, Vol. 132(1), 2006, pp. 1-11.
[23] Shinoda, M., and Bathurst, R. J., Strain measurement of geogrids using a video-extensometer technique. Geotechnical testing journal, Vol. 27(5), 2005, pp. 456-463.
[24] Stanier, S. A., Blaber, J., Take, W. A., and White, D. J., Improved image-based deformation measurement for geotechnical applications. Canadian Geotechnical Journal, Vol. 53(5), 2015, pp. 727-739.
[25] Mishra, S. R., Nithin, S., Mohapatra, S. R., and Rajagopal, K., Application of Image Processing Technique in Wide Width Tensile Testing of Nonwoven Geotextile. In Sixth Asian Regional Conference on Geosynthetics, New Delhi, India, International Geosynthetics Society, Jupiter, FL, 2016, pp. 795-803.
[26] Pan, B., Qian, K., Xie, H., and Asundi, A., Two-dimensional digital image correlation for in-plane displacement and strain measurement: a review. Measurement science and technology, Vol. 20(6), 2009, pp. 062001.
[27] Rajapakse, J., Gallage, C., Dareeju, B., Madabhushi, G., and Fenner, R., Estimation of Poisson's Ratio and Variation of Tensile Yield Strength of Composite Clay Balls Used in Pebble Matrix Filtration. Journal of Materials in Civil Engineering, Vol. 29(9), 2017, pp. 04017107-1-8
[28] Thamboo, J. A., Dhanasekar, M., and Yan, C., Effects of joint thickness, adhesion and web shells to the face shell bedded concrete masonry loaded in compression. Australian Journal of Structural Engineering, Vol. 14(3), 2013, pp. 291-302.
[29] Sveen, J. K., and Cowen, E. A., Quantitative imaging techniques and their application to wavy flows. In PIV and water waves, 2004, pp. 1-49.
[30] White, D. J., Take, W. A., and Bolton, M. D., Soil deformation measurement using particle image velocimetry (PIV) and photogrammetry. Geotechnique, Vol. 53(7), 2003, pp. 619-631.
[31] Taylor, Z. J., Gurka, R., Kopp, G. A., and Liberzon, A., Long-duration time-resolved PIV to study unsteady aerodynamics. IEEE Transactions on Instrumentation and Measurement, Vol. 59(12), 2010, pp. 3262-3269.
[32] Thielicke, W., and Stamhuis, E.J., PIVlab – towards user-friendly, affordable and accurate digital particle image velocimetry in MATLAB. Journal of Open Research Software, 2014, 2(1): e30

Copyright © Int. J. of GEOMATE. All rights reserved, including the making of copies unless permission is obtained from the copyright proprietors.